

PCCP

Accepted Manuscript



This is an *Accepted Manuscript*, which has been through the Royal Society of Chemistry peer review process and has been accepted for publication.

Accepted Manuscripts are published online shortly after acceptance, before technical editing, formatting and proof reading. Using this free service, authors can make their results available to the community, in citable form, before we publish the edited article. We will replace this *Accepted Manuscript* with the edited and formatted *Advance Article* as soon as it is available.

You can find more information about *Accepted Manuscripts* in the [Information for Authors](#).

Please note that technical editing may introduce minor changes to the text and/or graphics, which may alter content. The journal's standard [Terms & Conditions](#) and the [Ethical guidelines](#) still apply. In no event shall the Royal Society of Chemistry be held responsible for any errors or omissions in this *Accepted Manuscript* or any consequences arising from the use of any information it contains.

Cite this: DOI: 10.1039/c0xx00000x

www.rsc.org/xxxxxx

ARTICLE TYPE

Properties of two-dimensional insulators: a DFT study of Co adsorption on NaCl and MgO ultrathin films

Hsin-Yi Tiffany Chen^a and Gianfranco Pacchioni*^a

Received (in XXX, XXX) Xth XXXXXXXXX 20XX, Accepted Xth XXXXXXXXX 20XX

DOI: 10.1039/b000000x

Recent experimental and theoretical results have shown that Co atoms deposited on ultrathin NaCl films grown on Au(111) result in spontaneous substitutional doping of the two-layers insulating material (Li et al. *Phys. Rev. Lett.* **2014**, *112*, 026102). This result opens the general question of the reactivity of transition metal (TM) atoms with ultrathin films consisting of few atomic layers. In this article, density functional theory with and without dispersion corrections has been used to compare the adsorption of Co atoms on various sites of unsupported and supported NaCl and MgO two-layer (2L) films. We found that Co interacts strongly with NaCl/Au(111) 2L films, and that Co incorporation in interstitial positions between the first and second NaCl layers is thermodynamically preferred compared to adsorption on the surface sites. Differently from NaCl, Co adsorbs preferentially on top of O in both unsupported and supported MgO 2L films. Co incorporation in the interstitial sites of MgO is highly unfavorable. These results show that the reactivity of TM atoms like Co is completely different on NaCl or MgO ultrathin films. The reasons for this difference, the role of dispersion, and the peculiar properties of two-dimensional insulators are discussed.

Introduction

Deposition of gas-phase metal atoms on the surface of insulating or semiconducting materials is important for the investigation of the mechanisms of diffusion, nucleation, growth and stabilization of supported metal nanoparticles.¹⁻⁴ These systems find applications on a variety of advanced technologies, like sensors, heterogeneous catalysts,⁵⁻⁶ in plasmonics and other optical devices based on nanoparticles,⁷ in magnetic systems at the nanoscale,⁸ etc. The characterization of these systems at an atomic level is, however, complicated by the insulating nature of the supports. To circumvent this problem, thin and ultrathin films of insulating materials are usually grown on a metal, thus allowing the use of techniques like scanning tunneling microscopy (STM) or photoemission where a conducting substrate is required.⁵ However, insulators at the nanoscale, forming truly two-dimensional structures, can exhibit properties and behaviors completely different from their bulk counterparts.⁹ Here we show an example of these peculiar properties by considering two classical insulating materials, NaCl and MgO.

NaCl is the prototype of ionic crystals, it has a well defined crystal structure and a wide band gap of 9 eV.¹⁰ NaCl ultrathin films¹¹⁻¹⁵ have been used as inert barriers to decouple the conduction band electrons of the metal support from the valence

states of adsorbed atoms (e.g., Ag, Au),¹⁶⁻¹⁷ molecules¹⁸⁻¹⁹ or nanostructures (e.g. C₆₀).²⁰⁻²¹ This has allowed to study interesting phenomena like the selective charging and discharging of supported metal atoms by electron injection from an STM tip.¹⁷ Recently, it has been shown that Co atoms adsorbed at low temperature on NaCl/Au(111) films result in spontaneous doping and incorporation into the NaCl layer.²² STM images combined with DFT calculations have revealed that Co atoms can replace both Na and Cl ions in the topmost layer of the NaCl/Au(111) film. DFT calculations also suggest the possibility for the Co atoms to penetrate into the surface layer of the NaCl film and to be stabilized in interstitial sites (interstitial doping).²³ This opens several questions. How the properties of a two-layer film differ from those of the corresponding surface of the bulk material? Is the capability to incorporate atoms typical of every two-dimensional insulator or is material dependent? What is the role of the support and the interface in determining the properties of two-dimensional insulators? How important is the level of theoretical treatment to address these kinds of interactions? To answer these questions we have compared the properties of supported and unsupported NaCl ultrathin films with those of the corresponding MgO structures.

MgO is the typical example of ionic oxide. It has the same cubic structure of NaCl and a band gap which is only slightly smaller, 7.8 eV.¹⁰ MgO ultrathin films have been deposited on substrates like Ag(100) or Mo(100) because of the relatively

^a Dipartimento di Scienza dei Materiali,

Università di Milano-Bicocca, via Cozzi 55, 20125 Milano, Italy

Tel: +39-2-64485219; E-mail: gianfranco.pacchioni@unimib.it

good lattice mismatch and their properties have been studied in detail.²⁴⁻³⁰ Recently, large homogeneous and defect poor MgO islands have been prepared on Ag(100) by adopting a new synthetic approach, showing the possibility to prepare these films with more control.³¹ Adsorption of metal atoms and clusters on MgO ultrathin films has also been considered extensively both theoretically and experimentally, with the aim to study chemical, optical and magnetic properties.^{5-6, 32} Co atoms deposited on MgO/Ag(100) have been used recently to study the magnetic anisotropy of single atom magnets.⁸

Co atoms interaction with NaCl and MgO supports will be investigated based on DFT calculations to unravel some general properties of these systems and to produce new general concepts. In particular, four aspects are of interest in this study. On a methodological side, the observed tendency of Co to be incorporated into NaCl supported films raises the question of the importance of van der Waals (vdW) interactions for this kind of bonding. In fact, a metal atom incorporated into an interstitial cavity of a host crystal can establish several direct dispersive interactions with the neighboring atoms. If these interactions are overestimated, this could result in an artificial stabilization of the atom in these sites. To this end we have systematically compared results obtained at the DFT level with results where dispersion interactions are included explicitly (DFT-D) using two slightly different formulations of the interacting potential. From this comparison we will learn about the role of dispersion forces for this kind of interactions.

The second aspect is related to the adsorption properties of the surface of bulk NaCl and bulk MgO crystals with those of a corresponding free-standing film containing two mono-layers (2L). The surface of bulk materials has been modeled by 3L NaCl and MgO films where the bottom layer is fixed at the bulk positions. This represents properly the real (100) surface of the bulk material. Previous work has shown that the adsorption properties are well converged with three layers of insulating material.³³⁻³⁴ In the case of 2L films we describe the reactivity of a hypothetical free-standing, fully optimized, two-dimension insulator. We also want to compare the behavior of NaCl and MgO. The different lattice parameters and ionic charges of these two systems could and do result in different adsorption behavior. The fourth and last question that we will try to answer is to what extent the properties of two-dimensional insulating layers depend on the formation of an interface with the supporting metal. In other words, do 2L NaCl and MgO films exhibit similar behaviors towards Co adsorption when free-standing or when supported on Au(111) and Ag(100) metals, respectively? This question is quite difficult to answer experimentally in a direct way, while a theoretical approach can provide very clear answers.

The paper is organized as follows. After the description of the computational details, we discuss the influence of vdW forces on the adhesion of the insulating NaCl and MgO films to the metal substrate. Next, we compare the Co atoms adsorption and incorporation into the NaCl (100) and MgO (100) surfaces. The following is dedicated to the adsorption on the free-standing 2D systems. Then we address the effect of the metal/insulator interface by comparing NaCl and MgO 2L films with the NaCl/Au(111) and MgO/Ag(100) counterparts. Conclusions are reported in the last section.

Computational details

Spin-polarized DFT calculations were performed using the generalized gradient approximation (PBE functional³⁵) and the plane waves code VASP.³⁶⁻³⁷ The interaction between the ions and the valence electrons is described by the projector augmented wave (PAW) method.³⁸ The kinetic energy cutoff for the plane-wave expansion was set to 400 eV. Since we are dealing with insulating materials (NaCl and MgO), one could wonder if the use of a standard generalized gradient approximation (GGA) functional is appropriate. In fact, it is well known that GGA calculations, due to the self-interaction error, underestimate band gaps. This could lead also to an incorrect band alignment in metal/insulator interfaces. However, we have shown recently for similar systems that the use of hybrid functionals results in different absolute values of the adsorption energies but does not change the physical picture emerging from simple GGA calculations.³⁹

The experimental NaCl bulk lattice constant, 5.64 Å (at 293K),⁴⁰ is well reproduced by the calculations at the PBE level (5.65 Å).⁴¹⁻⁴² The (100) surface of bulk NaCl has been modeled by a 3L NaCl slab with the bottom layer fixed at the bulk positions. The lattice constant of 2L NaCl films shrinks to 5.54 Å at the PBE level; this value is used also for the supported films (see below). The NaCl films on Au(111) substrates have been modeled by a coincidence structure, obtained by superposing a (2 × 2) NaCl(100) unit cell on a $\begin{pmatrix} 3 & 1 \\ 1 & 3 \end{pmatrix}$ superstructure of the Au(111) surface, consisting of 4 NaCl units or 8 Au atoms per layer.^{22, 43} This coincidence structure presents a residual strain of about 5%, which is accommodated in the gold substrate, while the angle of the substrate unit cell is adjusted from 82° to 90° to match the square symmetry of the NaCl film. Therefore, the same lattice parameter, 5.54 Å, is applied for the unsupported and supported NaCl films. This allows us to compare directly the role of the supporting metal on the properties of the NaCl 2L films. The Au surface is modeled by a five atomic layer thick slab. A (6 × 6 × 1) Monkhorst-Pack grid is used for the reciprocal space sampling. The atomic coordinates of the top-three-layers of the Au slab and all the coordinates of the NaCl film and Co atoms are fully relaxed.

The (100) surface of bulk MgO is represented by a MgO 3L film (bottom layer fixed, as for NaCl). This approach has been followed in previous studies and provides a robust representation of the surface properties of bulk MgO.³³⁻³⁴ The experimental lattice constant of Ag (4.09 Å)⁴⁴ is about 3% smaller than that of MgO (4.21 Å).⁴⁵ In the calculations, the optimized Ag and MgO lattice parameters are 4.17 and 4.26 Å, respectively, and their lattice mismatch is reduced to about 2%. Here, the MgO film is adapted to the Ag lattice and is slightly contracted when supported on Ag. The O and Mg atoms are located on top of Ag atoms and on the hollow sites respectively.²⁹ During the geometry optimization of the MgO/Ag(100) interface, all atoms in the MgO film and in the two outmost Ag layers were relaxed, while the remaining two metal layers are frozen at the bulk positions. A surface (3 × 3) supercell was employed, containing 9 MgO units or Ag atoms per layer, and a (4 × 4 × 1) Monkhorst-Pack grid was used for the k-point sampling. The fact that the strain between supporting metal and thin film is accommodated on the metal (NaCl/Au) or on the insulating layer (MgO/Ag) is due to

the different faces of metal crystal exposed, (111) for Au and (100) for Ag. With the adopted procedure the atomic rearrangements at the metal/insulator interface are minimized.

Atomic charges are obtained within the scheme of charge density decomposition proposed by Bader.⁴⁶ The reported magnetic moments are the total magnetic moments per unit cell.

The inclusion of van der Waals (vdW) interactions is particularly important since the adhesion of the NaCl or MgO films to the metal support is dominated by polarization and dispersion forces. vdW forces can be important also for the adsorption of metal atoms on an insulating film. In this work, dispersion has been included by using the pair-wise force field implemented by Grimme (DFT-D2).⁴⁷ This approach is not free from limitations; for instance, the metallic screening of the dispersive interactions is not considered in the pair-wise evaluation of dispersion forces and leads to an overestimation of the interaction energies.⁴⁸ In a slightly different approach, PBE-D2', the C_6 parameters and van der Waals Radii R_0 of Na and Mg have been replaced by those of Ne since the size of this atom is closer to that of the Na^+ and Mg^{2+} cations.

The binding energy of a Co atom is defined as

$$E_b = E(\text{Co/MX/metal}) - E(\text{Co}) - E(\text{MX/metal}) \quad (1)$$

where M = Na or Mg, X = Cl or O, metal = Au or Ag. The same formula applies for unsupported films (in this case the metal is absent). $E_b < 0$ indicates an exothermic process.

Results and discussion

Role of van der Waals forces on the metal/oxide adhesion energy

We discuss first the role of vdW forces on the adhesion of the insulating NaCl or MgO films to the metal surface. The properties of interest are the adhesion energy and the interface distance; this latter is defined as the distance between the average vertical position of the atoms in the top layer of the metal support and that of the bottom layers of cation and anion sublattices in the insulating film, Table 1. The adhesion energy is defined as,

$$E_{\text{adhesion}} = [E(\text{MX/metal}) + E(\text{metal}) - E(\text{MX/metal})]/S \quad (2)$$

where M = Na or Mg, X = Cl or O, metal = Au or Ag, and S is the surface area of the supercell in \AA^2 . $E_{\text{adhesion}} > 0$ indicates a bound interface.

Table 1 Interface distance, d (\AA), and adhesion energy, E_{adhesion} ($\text{meV}/\text{\AA}^2$), for NaCl/Au(111) and MgO/Ag(100) interfaces.

		PBE	PBE-D2	PBE-D2'
MgO(2L)/Ag(100)	d , \AA	3.50	2.95	3.12
	E_{adhesion} , $\text{meV}/\text{\AA}^2$	8.5	37.9	25.5
NaCl(2L)/Au(111)	d , \AA	2.70	2.53	2.62
	E_{adhesion} , $\text{meV}/\text{\AA}^2$	22.5	76.1	46.9

The role of dispersion forces is important in both NaCl/Au(111) and MgO/Ag(100) systems, but it has a stronger impact on the description of NaCl/Au(111). The NaCl-Au

interface distance, in fact, changes from 3.50 \AA at the PBE level to about 3 \AA after inclusion of dispersion. PBE-D2 overestimates the contribution of vdW forces, resulting in a distance of 2.95 \AA , while PBE-D2' gives a slightly larger interface distance, 3.12 \AA , Table 1. Regarding the adhesion energy, the values using PBE-D2 and PBE-D2' are about 3-4 times larger than the PBE one. E_{adhesion} at the PBE-D2 level, 37.9 $\text{meV}/\text{\AA}^2$, is about 50% larger than at the PBE-D2' level, 25.5 $\text{meV}/\text{\AA}^2$.

This trend is found also for MgO/Ag(100) but the changes of the interface distance are less pronounced. In particular, going from the PBE approach to PBE-D2' the change in interface distance is 0.08 \AA only. The results at the PBE level are in line with other values reported in the literature and obtained at the same level of theory.⁴⁹⁻⁵⁰ The PBE-D2 calculation, 2.53 \AA , is consistent with the results obtained by Ling et al.⁵⁰ with the same method giving a Ag-O distance of 2.50 \AA and with another theoretical study using a localized basis set.⁵¹ As we mentioned before, the combination of PBE-D2 with Na or Mg cations is likely to overestimate the dispersion interaction. Indeed, it has been reported that the inclusion of the Grimme's D3 correction,⁵² which is less empirical than the D2 approach, gives an Ag-O distance of 2.62 \AA .⁵⁰ This latter value coincides with that obtained here using the PBE-D2' method, Table 1. Experimentally, the reported interface distance for MgO/Ag(001) is between 2.39 and 2.53 \AA .⁵³⁻⁵⁵ Although the interface distances computed with the three schemes vary slightly, the adhesion energies obtained with PBE-D2 and PBE-D2' are much larger than the PBE one, Table 1. The results show that the PBE-D2' adhesion energy of MgO 2L films with the Ag substrate is twice that of the NaCl 2L film with the Au substrate. Such strong change in adhesion energy is also reflected in the interface distance: at the PBE-D2' level the NaCl/Au separation, 3.12 \AA is 0.5 \AA longer than the MgO/Ag one, Table 1.

Co adsorption on bulk NaCl(100) and MgO(100) surfaces

In this section we discuss the adsorption properties of a single Co atom on the terraces of non-defective NaCl(100) and MgO(100) surfaces. The model consists of a three-layer slab. Co atoms have been placed on top of cations (Na and Mg) and anions (Cl and O), on hollow position and in an interstitial site, Table 2. The adsorption on top of Na and Mg cations are not minima and will not be further discussed.

On NaCl(100) Co adsorbs with not too different energies on top of Cl or in hollow sites, Table 2. In particular, the PBE binding energy is -0.74 eV and -0.87 eV, respectively. Inclusion of dispersion increases the binding (in absolute value) and results in similar binding energies at the PBE-D2 level (-0.94 versus -0.93 eV, respectively). At the PBE-D2' level the order of stability is the same as for PBE with the Cl-top site bound by -0.82 eV and the hollow site slightly more stable, -0.90 eV. In all cases the Co atom remains neutral, as shown by the Bader charges, and the bonding originates from the mixing of the Co 3d states with the Cl 3p orbitals. If the Co atom is introduced in an interstitial site between the first and the second NaCl layers, the system undergoes a geometrical distortion that involves mainly the top NaCl layer resulting in a configuration where Co is bound by 1 eV or more, depending on the method, Table 2. At the PBE level the bonding is -0.97 eV, and increases to -1.37 and -1.18

eV at the PBE-D2 and PBE-D2' levels, respectively. Therefore, the binding energy in this configuration is larger than for adsorption on the surface, Table 2. This does not mean that spontaneous incorporation of Co in sub-surface sites is expected since on the surface of NaCl the process is certainly accompanied

Table 2 Binding energies, E_b (eV), and Bader charge, q ($|e|$), for a Co atom adsorbed or incorporated on the surface of NaCl and MgO (100) 3L films, and on unsupported and supported NaCl and MgO 2L films.

			Anion-top	Hollow	Interstitial
NaCl(100) (3L)	E_b	PBE	-0.74	-0.87	-0.97
	E_b	PBE-D2	-0.94	-0.93	-1.37
	E_b	PBE-D2 ^(a)	-0.82	-0.90	-1.18
	q	PBE-D2'	-0.07	-0.06	-0.02
MgO(100) (3L)	E_b	PBE	-1.49	^(b)	-0.05 ^(c)
	E_b	PBE-D2	-1.81	^(b)	-0.30 ^(c)
	E_b	PBE-D2 ^(a)	-1.66	^(b)	-0.29 ^(c)
	q	PBE-D2'	-0.15	-	0.80 ^(c)
NaCl film (2L)	E_b	PBE	-0.70	-0.88	-1.14
	E_b	PBE-D2	-0.89	-1.02	-1.59
	E_b	PBE-D2 ^(a)	-0.78	-0.93	-1.36
	q	PBE-D2'	-0.06	-0.04	-0.03
MgO film (2L)	E_b	PBE	-1.45	^(b)	1.11
	E_b	PBE-D2	-1.76	^(b)	1.14
	E_b	PBE-D2 ^(a)	-1.62	^(b)	0.94
	q	PBE-D2'	-0.03	-	-0.11
NaCl(2L)/Au (111)	E_b	PBE	-1.07	-2.57	-3.09
	E_b	PBE-D2	-1.13	-2.58	-3.22
	E_b	PBE-D2 ^(a)	-1.06	-2.55	-2.98
	q	PBE-D2'	0.25	0.44	0.63
MgO(2L)/Ag (100)	E_b	PBE	-1.40	-	-0.17
	E_b	PBE-D2	-1.72	-	-0.47
	E_b	PBE-D2 ^(a)	-1.45	-	-0.33
	q	PBE-D2'	-0.09	-	0.60

(a) PBE-D2': the C_6 parameters and van der Waals Radii R_0 of Na and Mg are replaced by those of Ne.

(b) Co goes to on top of O.

(c) Co goes in a Mg substitutional site and displaces the Mg atom which moves to a bridge adsorption site

by an energy barrier (not investigated here). Notice that in the interstitial site Co remains neutral, since no electron transfer is possible from the valence states of Co to the high lying conduction band states of the NaCl film (in a perfect film there are no other acceptor levels available).

When we consider Co adsorption on MgO(100) we notice that Co binds on top of O with a binding energy of about -1.5/-1.8 eV, depending on the approach, Table 2. This is about twice E_b on NaCl(100). The hollow site is not a minimum, at variance with NaCl. Also in this case the bonding of Co is due to the hybridization of the Co 3d and O 2p valence states, with moderate electron transfer from the "basic" MgO surface to Co (Bader charge -0.15 e). Things are totally different when Co is placed in an interstitial position between the first and the second layers of the MgO(100) surface. The site is clearly too small to accommodate the Co atom, which thus moves to the Mg lattice

position giving rise to a substitutional doping of the MgO surface layer. A Mg atom is displaced to the surface where it is adsorbed on a Co-O bridge site. The final configuration is thus that of a Mg atom adsorbed on a Co-doped MgO surface. This phenomenon is independent of the inclusion of vdW forces. The Co atom becomes positively charged since it takes a cation position in the lattice of the ionic crystal. However, the total energy of this configuration is about 1.4-1.5 eV higher than for Co adsorbed on top of O.

To summarize this part, from a thermodynamic point of view we have two quite different situations for a Co atom adsorbed on the surface of NaCl(100) and MgO(100) ionic crystals. In fact, on NaCl the interstitial site is the most stable one while on MgO is totally unfavorable and only surface adsorption is possible. This result is due to the fact that the interstitial cavity in NaCl is considerably larger than in MgO, due to the different lattice constants of the two materials, 5.64 Å NaCl, 4.21 Å MgO.

Based on Table 2, we can draw some conclusions about the importance of dispersion interactions for the adsorption properties of Co atoms on NaCl and MgO supports. In general, dispersion interactions increase the adsorption energy (in absolute value), an effect which is more pronounced at the PBE-D2 level. At the PBE-D2' level the increase in adsorption energy for the surface sites is smaller than 0.1 eV. The effect on the interstitial sites is different. Here we notice that at the PBE-D2 level the increase in binding energy is substantial, 0.4 eV. This is the consequence of the interaction of the Co atom with several neighbors. The role of dispersion is less pronounced when we use the PBE-D2' approach where the vdW forces contribute about 0.2 eV to the total binding. These conclusions, obtained for the unsupported 3L NaCl(100) and MgO(100) surfaces, are valid also for the other systems considered, Table 2. An important conclusion is that the relative stability of the adsorption sites considered does not change upon inclusion of dispersion. Also the absolute values of E_b are not too different at the DFT or at the DFT-D levels. Therefore, in the following we will discuss adsorption energies obtained with the more accurate PBE-D2' level, but values obtained at PBE and PBE-D2 levels are reported for completeness in Table 2.

Co adsorption on free-standing NaCl and MgO 2L films

The order of stability for Co adsorption on an unsupported, free-standing NaCl 2L film is interstitial > hollow > on top of Cl, Table 2 and Fig. 1. At the DFT-D2' level the two adsorption energies on the surface (on top of Cl and hollow) are quite similar, -0.78 and -0.93 eV, respectively. An energy gain of 1.36 eV is found when the Co atom is in an interstitial position, Table 2 and Fig. 1. Thus, the order of stability is the same found for Co adsorbed on the 3L NaCl(100) surface discussed above. Also the absolute values of the adsorption energies are similar, Table 2. This reflects the fact that the bonding with the Co atom has the same nature on the bare surface (3L film) and on the free-standing 2L film. In particular, Co remains essentially neutral or is slightly negatively charged, as shown by the Bader charges, Table 2.

Things are quite different when MgO is considered. As for the MgO(100) surface, also on the 2L film there is only one stable Co adsorption site, on top of O, with an adsorption energy of -1.62

eV, and the value of E_b is similar to that computed for the 3L MgO(100) surface (-1.66 eV). The hollow site is not a minimum and when the geometry optimization starts from this position the Co atom moves spontaneously to the O-top site. A metastable structure is found when Co is included in the interstitial position.

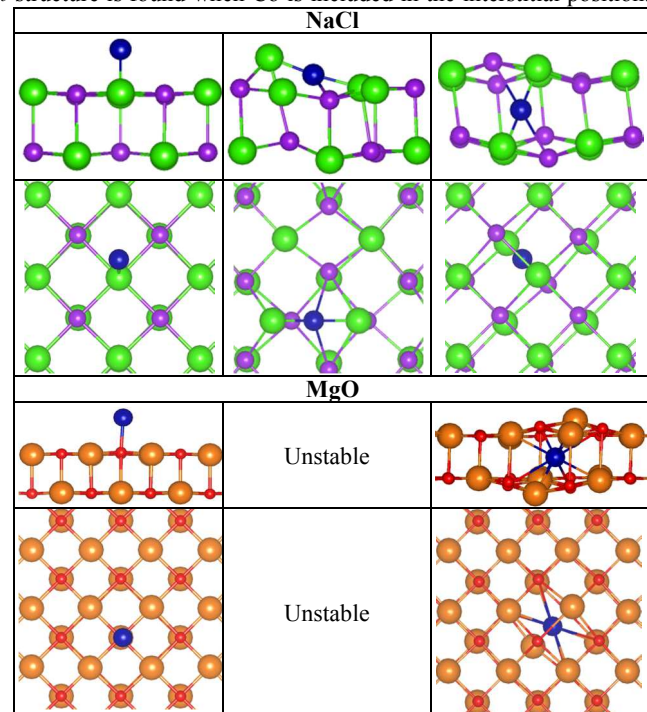


Fig. 1 Side and top views of a Co atom adsorbed on top of the anion (left), in hollow sites (center), or in interstitial sites (right) of free standing NaCl (top) and MgO (bottom) 2L films (blue: Co; violet: Na; green: Cl; orange: Mg; red: O)

10

The structure of the 2L film undergoes a substantial distortion to accommodate the extra atom, see Fig. 1. The distortion of the film allows to partially accommodate the strain so that no spontaneous displacement of the Mg ion from its lattice position occurs, in contrast with the MgO(100) case. However, in this configuration the system is unbound by 0.94 eV, indicating a strong steric repulsion. Another configuration exists with the Co atom replacing Mg in the film as found for the MgO(100) surface, but this is about 1.5 eV less stable than the ground state (Co on top of O).

In both NaCl and MgO films the Co atom keeps the same number of electrons it has in the free state and remains essentially neutral, Table 2. This is because there are no acceptor states in non-defective NaCl or MgO films to accommodate extra electrons coming from the adsorbed atom. This makes the formation of a cation, Co^{n+} , energetically unfavorable. Therefore, the results of Co adsorption on free-standing NaCl and MgO 2L films show a preference for the same adsorption sites as for the corresponding bulk surfaces (3L films). Co binds on the surface of MgO and shows no tendency to be incorporated into the two-dimensional MgO 2L film. On NaCl the situation is different and the thermodynamically stable structure is with the Co atom adsorbed between the first and the second NaCl layers.

In ultimate analysis, the different behavior of NaCl and MgO

can be traced back to the much stronger Madelung potential in the oxide compared to the chloride and, to minor extent, also to the larger strain in NaCl/Au compared to MgO/Ag. The formation of a crystal with M^{2+} and X^{2-} ions leads to an electrostatic attraction which, for the same crystal structure and ion separation, is four times larger that of an ionic solid composed of mono-valent M^+ and X^-

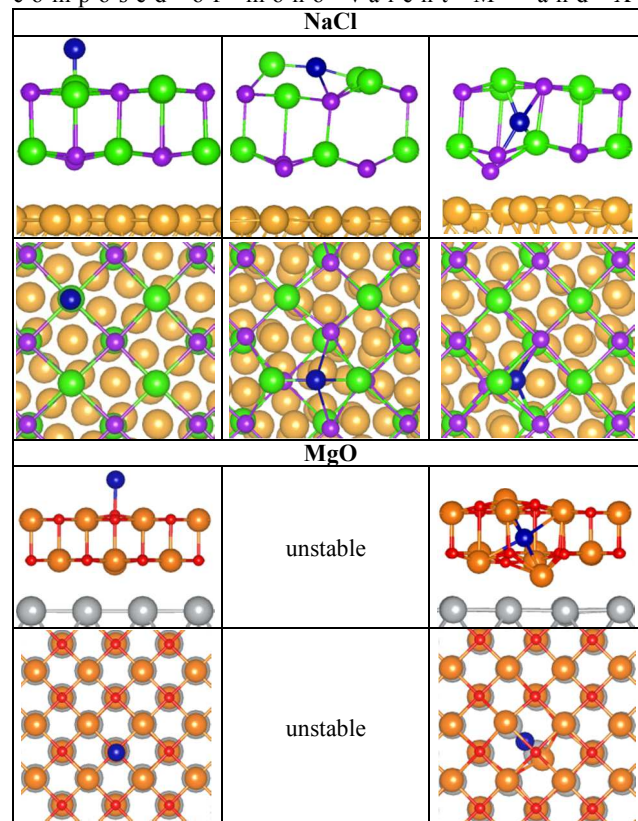


Fig. 2 Side and top views of a Co atom adsorbed on top of the anion (left), in hollow sites (center), or in interstitial sites (right) of NaCl/Au(111) (top) and MgO/Ag(100) (bottom) 2L films (blue: Co; violet: Na; green: Cl; gold: Au; orange: Mg; red: O; grey: Ag)

ions. Thus, the forces required to “open” the structure and incorporate the TM atom are much stronger in MgO than in NaCl. This, associated to the shorter lattice parameter explains the quite different reactivity of the two substrates.

55 Co adsorption on supported NaCl(2L)/Au(111) and MgO(2L)/Ag(100) films

In this section we consider Co adsorption on 2L NaCl and MgO films deposited on Au(111) and Ag(100) supports, respectively, Fig. 2. In both cases the structures of the NaCl/Au(111) and MgO/Ag(100) interfaces have been fully optimized keeping only the two metal bottom layers fixed. As discussed above the insulating film interacts largely via dispersion forces with the metal support. This could suggest that the adsorption properties of the NaCl and MgO films are very similar with or without the metal support. This is not necessarily the case, and the reasons are discussed below.

The adsorption properties of Co on NaCl/Au(111) films are drastically different from those of the unsupported NaCl layer. For adsorption on top of Cl, E_b increases slightly, from -0.78 eV (unsupported) to -1.06 eV (supported), Table 2. On the other hand, the adsorption on the hollow site of NaCl/Au(111) is completely different and leads to an energy gain of 2.55 eV, nearly three times that found on the unsupported NaCl 2L film, Table 2. In both cases the top NaCl layer undergoes a major reconstruction (see Fig. 1 and Fig. 2). The reason for the larger Co adsorption energy on NaCl/Au(111) is related to the different nature of the interaction. On NaCl/Au(111) the presence of the metal Fermi level which falls within the band gap of the insulating NaCl film offers the possibility to transfer the valence electrons of the Co adsorbate to the Au support, with formation of a Co^{nt} species. This leads to a charge transfer interaction with considerable reinforcement of the bond. In fact, while on the free-standing NaCl 2L film the Bader charge on Co is slightly negative, $q = -0.04$ e, when Co is adsorbed in the hollow site of NaCl/Au(111) it becomes positive, $q = 0.44$ e, Table 2.

This effect becomes very important when incorporation into the interstitial site is considered. While in the unsupported 2L film Co interstitial is bound by 1.36 eV and is neutral ($q = -0.03$ e), on NaCl/Au(111) the binding becomes nearly -3 eV and the charge $q = 0.63$ e, Table 2. Due to the strong interaction, the role of van der Waals forces is negligible. The adsorption is accompanied by a major geometrical relaxation, with displacement of a Na ion in the second NaCl layer towards the Au(111) support, Fig. 2. The supported NaCl/Au(111) 2L film is very flexible and is able to incorporate the Co atom with a large energy gain. Co donates charge to the support forming a Co^+ ion with consequent reduction of the steric repulsion and increase of the electrostatic attraction. The final result is that the order of stabilities is the same for the unsupported and supported NaCl 2L films, interstitial > hollow > on top of Cl, but the adsorption energies and bonding modes are totally different. In particular, large energy gains are associated to the formation of Co cations on the NaCl/Au(111) supported films, an effect that cannot occur on the free-standing two-dimensional material. Beside this obvious difference, the supported NaCl films show also a greater tendency to distort compared to the bare NaCl(100) surface, possibly due to some attractive polarization interactions between the displaced ions of the film and the metal support. This large structural flexibility can be at the basis of interesting and unexpected properties of NaCl ultrathin films.

Now we consider Co adsorption on MgO/Ag(100) 2L films. As for NaCl/Au(111), in Table 2, we notice that the role of the van der Waals forces is negligible. Compared to the free standing film, Co adsorption on top of O remains the most stable configuration. Also the adsorption energy, -1.45 eV, is close to that found on the unsupported MgO case, -1.62 eV. This similarity in binding energy reflects a similar bonding nature in the two cases. Co binds via covalent polar bonds, with only moderate charge transfer due to the hybridization of the Co 3d and the O 2p levels. The Bader charges are very close for the three cases examined, MgO(100), MgO 2L film, and MgO(2L)/Ag(100), and are slightly negative, Table 2. In this respect, the presence of the Ag support is irrelevant, and the supported or unsupported films behave essentially in the same

way.

This is no longer true when the adsorption in interstitial sites is considered. Here in fact one goes from a highly unfavorable, endothermic adsorption on the unsupported MgO 2L film ($E_b = +0.94$ eV), to a slightly exothermic interaction for MgO(2L)/Ag(100), -0.33 eV, Table 2. The energy gain due to the Ag support is thus of about 1.4 eV. This is more or less the same energy difference found for Co included in interstitial sites going from NaCl 2L to NaCl/Au(111) films (here the adsorption energy in the interstitial site goes from -1.36 to -2.98 eV, respectively, Table 2). The larger stability of the interstitial site of MgO/Ag(100) compared to 2L MgO is due to the occurrence of a net charge transfer from Co to the MgO/Ag(100) interface. In this latter case Co donates 0.6 valence electrons to the Ag metal, forms $\text{Co}^{\delta+}$ thus reducing the steric repulsion, with a mechanism similar to that observed for NaCl/Au(111). The difference is that on NaCl/Au(111) the interstitial site is the most stable one, while on MgO/Ag(100) the interstitial cavity is too small to accommodate the Co cation resulting in a strong steric repulsion. Adsorption on the surface of the film remains clearly preferred (-1.45 eV on top of O, -0.33 eV interstitial). Again, the different behavior of MgO compared to NaCl in the ultrathin limit can be attributed to the stronger Madelung field in the oxide compared to the chloride.

Conclusions

In recent years an increasing attention has been dedicated to the properties of two-dimensional crystals. Here we have discussed theoretical results obtained on two-dimensional ionic materials like NaCl and MgO. We have compared in particular the adsorption properties of Co atoms on three different supports: (1) models of a bulk NaCl or MgO(100) surface; (2) free-standing two-layer (2L) NaCl and MgO films; (3) metal supported 2L NaCl/Au(111) and MgO/Ag(100) films. While free standing NaCl and MgO layers are at the moment purely hypothetical, the bulk surfaces and the supported films are available for experimental investigations and have been studied quite intensively.

We found that while adsorption of Co atoms on bulk NaCl and MgO, and on free-standing 2L films present several similarities, this is no longer true when the ultrathin films are deposited on a metal support. The main difference is that on the perfect, defect free insulators no charge transfer is possible, while on the supported films the Co atoms can donate charge to the metal support, changing completely the adsorption properties. Furthermore, the supported films are more flexible and easy to distort than the bare materials. As a consequence, incorporation of a transition metal atom in the interstitial sites of NaCl becomes preferred compared to adsorption on the surface of the film. This is not true for MgO where adsorption on the surface is always more stable than incorporation in interstitial sites. These results have been checked also by including dispersion forces, showing that the results are essentially independent of these interactions. The completely different behaviour of NaCl and MgO two-dimensional ionic crystals can be related to the larger Madelung potential in the oxide compared to the chloride.

Acknowledgment

Financial support from the Italian MIUR through the FIRB Project RBAP115AYN is gratefully acknowledged.

References

1. A. T. Bell, *Science*, 2003, **299**, 1688-1691.
2. J. Libuda and H. J. Freund, *Surf Sci Rep*, 2005, **57**, 157-298.
3. M. Salmeron and R. Schlogl, *Surf Sci Rep*, 2008, **63**, 169-199.
4. G. A. Somorjai and J. Y. Park, *Chem Soc Rev*, 2008, **37**, 2155-2162.
5. H. J. Freund and G. Pacchioni, *Chem Soc Rev*, 2008, **37**, 2224-2242.
6. G. Pacchioni and H. Freund, *Chem. Rev.*, 2013, **113**, 4035-4072.
7. J. A. Fan, C. H. Wu, K. Bao, J. M. Bao, R. Bardhan, N. J. Halas, V. N. Manoharan, P. Nordlander, G. Shvets and F. Capasso, *Science*, 2010, **328**, 1135-1138.
8. I. G. Rau, S. Baumann, S. Rusponi, F. Donati, S. Stepanow, L. Gragnaniello, J. Dreiser, C. Piamonteze, F. Nolting, S. Gangopadhyay, O. R. Albertini, R. M. Macfarlane, C. P. Lutz, B. A. Jones, P. Gambardella, A. J. Heinrich and H. Brune, *Science*, 2014, **344**, 988-992.
9. G. Pacchioni, *Chem-Eur J*, 2012, **18**, 10144-10158.
10. W. H. Strehlow and E. L. Cook, *Journal of Physical and Chemical Reference Data*, 1973, **2**, 163-200.
11. C. Bombis, F. Ample, J. Mielke, M. Mannsberger, C. J. Villagomez, C. Roth, C. Joachim and L. Grill, *Phys. Rev. Lett.*, 2010, **104**, 185502.
12. G. Cabailh, C. R. Henry and C. Barth, *New J. Phys.*, 2012, **14**, 103037.
13. H. C. Ploigt, C. Brun, M. Pivetta, F. Patthey and W. D. Schneider, *Phys Rev B*, 2007, **76**, 195404.
14. J. Repp, G. Meyer, S. Paavilainen, F. E. Olsson and M. Persson, *Phys. Rev. Lett.*, 2005, **95**, 225503.
15. M. Wagner, F. R. Negreiros, L. Sementa, G. Barcaro, S. Surnev, A. Fortunelli and F. P. Netzer, *Phys. Rev. Lett.*, 2013, **110**, 216101.
16. F. E. Olsson, S. Paavilainen, M. Persson, J. Repp and G. Meyer, *Phys. Rev. Lett.*, 2007, **98**, 176803.
17. J. Repp, G. Meyer, F. E. Olsson and M. Persson, *Science*, 2004, **305**, 493-495.
18. S. H. Kim, H. G. Jeong, S. J. Lim, U. D. Ham, Y. J. Song, J. Yu and Y. Kuk, *Surf Sci*, 2013, **613**, 54-57.
19. S. C. Yan, Z. J. Ding, N. Xie, H. Q. Gong, Q. Sun, Y. Guo, X. Y. Shan, S. Meng and X. H. Lu, *Acs Nano*, 2012, **6**, 4132-4136.
20. E. Čavar, M.-C. Blüm, M. Pivetta, F. Patthey, M. Chergui and W.-D. Schneider, *Phys. Rev. Lett.*, 2005, **95**, 196102.
21. F. Rossel, M. Pivetta, F. Patthey, E. Čavar, A. P. Seitsonen and W.-D. Schneider, *Phys Rev B*, 2011, **84**, 075426.
22. Z. Li, H. Y. T. Chen, K. Schouteden, K. Lauwaet, L. Giordano, M. I. Trioni, E. Janssens, V. Iancu, C. Van Haesendonck, P. Lievens and G. Pacchioni, *Phys. Rev. Lett.*, 2014, **112**, 026102.
23. H. Y. T. Chen, L. Giordano and G. Pacchioni, *J. Phys. Chem. C*, 2014, **118**, 12353-12363.
24. S. Schintke, S. Messerli, M. Pivetta, F. Patthey, L. Libioulle, M. Stengel, A. De Vita and W. D. Schneider, *Phys. Rev. Lett.*, 2001, **87**, 276801.
25. S. Valeri, S. Altieri, U. del Pennino, A. di Bona, P. Luches and A. Rota, *Phys Rev B*, 2002, **65**, 245410.
26. S. Benedetti, P. Torelli, S. Valeri, H. M. Benia, N. Nilius and G. Renaud, *Phys Rev B*, 2008, **78**, 195411.
27. M. C. Wu, J. S. Corneille, C. A. Estrada, J. W. He and D. W. Goodman, *Chem. Phys. Lett.*, 1991, **182**, 472-478.
28. J. Wollschlager, D. Erdos and K. M. Schroder, *Surf Sci*, 1998, **402-404**, 272-276.
29. M. Kiguchi, T. Goto, K. Saiki, T. Sasaki, Y. Iwasawa and A. Koma, *Surf Sci*, 2002, **512**, 97-106.
30. M. S. Chen and D. W. Goodman, *J. Phys.: Condens. Matter*, 2008, **20**, 264013.
31. J. Pal, M. Smerieri, E. Celasco, L. Savio, L. Vattuone and M. Rocca, *Phys. Rev. Lett.*, 2014, **112**, 126102.
32. L. Giordano and G. Pacchioni, *Acc. Chem. Res.*, 2011, **44**, 1244-1252.
33. G. Pacchioni, L. Giordano and M. Baistrocchi, *Phys. Rev. Lett.*, 2005, **94**, 226104.
34. L. Giordano, M. Baistrocchi and G. Pacchioni, *Phys Rev B*, 2005, **72**, 115403.
35. J. P. Perdew, K. Burke and M. Ernzerhof, *Phys. Rev. Lett.*, 1996, **77**, 3865-3868.
36. G. Kresse and J. Hafner, *Phys Rev B*, 1993, **47**, 558-561.
37. G. Kresse and J. Furthmuller, *Phys Rev B*, 1996, **54**, 11169-11186.
38. P. E. Blöchl, *Phys Rev B*, 1994, **50**, 17953-17979.
39. S. Prada, L. Giordano and G. Pacchioni, *J. Phys. Chem. C*, 2013, **117**, 9943-9951.
40. D. E. Gray (ed.), *American Institute of Physics Handbook*, McGraw-Hill, New York, 1972.
41. V. N. Staroverov, G. E. Scuseria, J. Tao and J. P. Perdew, *Phys. Rev. B* 2004, **69**, 075102.
42. P. Haas, F. Tran and P. Blaha, *Phys. Rev. B*, 2009, **79**, 085104.
43. K. Lauwaet, K. Schouteden, E. Janssens, C. Van Haesendonck, P. Lievens, M. I. Trioni, L. Giordano and G. Pacchioni, *Phys. Rev. B*, 2012, **85**, 245440.
44. N. W. Ashcroft and N. D. Mermin, *Solid State Physics*, John Wiley & Sons, New York, 1996.
45. A. R. West, *Basic Solid State Chemistry*, Wiley, New York, 1994.
46. R. F. W. Bader, *Chem. Rev.*, 1991, **91**, 893-928.
47. S. Grimme, *J. Comput. Chem.*, 2006, **27**, 1787-1799.
48. G. Mercurio, E. R. McNellis, I. Martin, S. Hagen, F. Leyssner, S. Soubatch, J. Meyer, M. Wolf, P. Tegeder, F. S. Tautz and K. Reuter, *Phys. Rev. Lett.*, 2010, **104**, 036102.
49. L. Giordano, F. Cinquini and G. Pacchioni, *Phys. Rev. B*, 2006, **73**, 045414.
50. S. L. Ling, M. B. Watkins and A. L. Shluger, *J. Phys. Chem. C*, 2013, **117**, 5075-5083.
51. A. M. Ferrari, *Surf Sci*, 2005, **584**, 269-277.
52. S. Grimme, J. Antony, S. Ehrlich and H. Krieg, *J. Chem. Phys.*, 2010, **132**, 154104.
53. A. M. Flank, R. Delaunay, P. Lagarde, M. Pompa and J. Jupille, *Phys Rev B*, 1996, **53**, R1737-R1739.
54. C. Giovanardi, A. di Bona, T. S. Moia, S. Valeri, C. Pisani, M. Sgroi and M. Busso, *Surf Sci*, 2002, **505**, L209-L214.
55. P. Luches, S. D'Addato, S. Valeri, E. Groppo, C. Prestipino, C. Lamberti and F. Boscherini, *Phys Rev B*, 2004, **69**, 045412.